Stewart, W. S., C. M. Sliepcevich, and T. H. Puckett, "Dynamics of Heat Removal from a Jacketed Agitated Vessel," *CEP Symp. Series*, 5 (36), 119 (1961).
Wood, R. K., and M. W. Berry, "Terminal Composition Control of a Binary Distillation Column," *Chem. Eng. Sci.*, 28, 1707 (1973).

Manuscript received March 26, 1979; revision received July 17, and accepted July 27, 1979.

Heat Transfer to a Stationary Sphere in a Plasma Flame

N. N. SAYEGH

and

W. H. GAUVIN

Department of Chemical Engineering
McGill University
Montreal, Quebec, Canada

The overall heat transfer rates to stationary spheres of highly-polished molybdenum (2 to 5.6 mm in diameter) in a confined argon plasma jet were experimentally measured. The effects of large temperature differences and large variations of the fluid property on the heat transfer process are investigated. The sphere Reynolds number range between 10 and 80, and the sphere temperature between 1,200 K and 2,400 K, with temperature differences between the gas and the sphere in excess of 2,000 K. These conditions are within the range commonly encountered in industrial plasma processing. The experimental values of the heat transfer coefficients are in reasonably good agreement with the predictions of a theoretical analysis of variable-property flow and heat transfer previously reported by the authors.

SCOPE

This study is part of a continuing program of investigation by the Plasma Technology Group to develop applications of plasmas to chemical and metallurgical processes of industrial interest. The availability of reliable plasma generating devices of industrial size (up to 10 MW) with a great deal of design flexibility is currently prompting a very active search to take advantage of some unique features that can lead to truly novel processes. Plasma systems offer continuous operation, ease of control, good energy utilization, and not the least important, an enormous concentration of energy in a very small volume, resulting in very high temperature levels and rates of throughput at or near atmospheric pressure. Heterogeneous solids-gas reactions involving the contacting of fine particles with an entraining plasma gas appear to be particularly promising in this regard.

The separation of refractory metals of high unit value (molybdenum, zirconium, tungsten, titanium, etc.) from concentrates of their ores; the production of valuable oxides (zirconia, TiO_2, ultra-pure silica); the production of ferroalloys (ferromolybdenum, ferrocolumbium, ferrovanadium); and the production of acetylene from coal are all examples of processes now under active investigation. However, due to the extremely short residence time of the particles in the high enthalpy plasma stream (typically, a few millisec), the design of a plasma reactor largely depends upon an accurate knowledge of the fluid mechanics and heat transfer characteristics of the system. The latter, in turn, enables the proper control of the thermal histories of the particles and consequently, of their degree of conversion. Comprehensive models to predict the temperature history of particles entrained in a plasma were presented by Boulos and Gauvin (1974) for a one-dimensional system, and by Bhattacharyya and Gauvin (1975) for a three-dimensional jet, using the thermal decomposition of MoS_2 into metallic molybdenum particles and elemental sulphur as an example in these simulations. Both studies emphasized the importance of heat transfer considerations in effecting the desired conversion.

Heat transfer to particles entrained by a plasma exhibits some unusual characteristics. First of all, the particle Reynolds number is remarkably low, typically less than 50, owing to the unusually high value of the plasma's kinematic viscosity. More important still, is the fact that in most heterogeneous plasma systems, the temperature of the particle may range from 1,500 to 2,500 K, while that of the surrounding plasma extends from 5,000 K upward. Under these conditions of very large temperature differences, it is no longer permissible to assume that the fluid immediately surrounding the particle exhibits constant properties, as is commonly done in more conventional situations at lower temperatures.

A theoretical study was recently published (Sayegh and Gauvin 1979) in which the effects of large temperature differences on the rate of pure heat transfer to a stationary

Sayegh is now at the Pulp and Paper Research Institute of Canada, Pointe Claire, Quebec. Gauvin is at the Noranda Research Centre, Pointe Claire, Quebec.

sphere are examined. From this numerical analysis, a heat transfer correlation was derived which accounted for the effects of large variations in the physical properties of the fluid as a result of these temperature differences.

This article describes an experimental study of pure heat transfer to a stationary sphere exposed to an argon plasma jet, which supports the theoretical predictions of the numerical analysis.

CONCLUSIONS AND SIGNIFICANCE

1. The rates of pure heat transfer from an argon plasma jet at temperatures up to 5,000 K to stationary spheres of polished molybdenum (2 to 5.6 mm in diameter) were experimentally measured, under conditions where a temperature difference of the order of about 2,000 K existed between the plasma stream and the sphere surface. The Reynolds number varied between 10 and 80.

2. The experimental results agreed reasonably well with the predictions of a theoretical study (Sayegh and Gauvin, 1979), in which the following correlation was derived

$$N_{Nu0} = 2f_0 + 0.473(N_{Pr})^m(N_{Re})^{0.552} \quad (1)$$

where

$$m = 0.78(N_{Re})^{-0.145} \quad (2)$$

and

$$2f_0 = 2(1 - T_0^{1+x})/[(1 + x)(1 - T_0)T_0^x] \quad (3)$$

The effects of the large variations in fluid properties, caused by the temperature difference, on the value of the Nusselt number are accounted for by introducing the variable-property limiting Nusselt number, $2f_0$, and by choosing suitable reference temperatures for the kinematic viscosity and thermal conductivity. The reference temperature for k is the sphere temperature, and that for ν is $T_{0.19} = T_s + 0.19\,(T_\infty - T_s)$. Thus N_{Nu} and hence the heat transfer coefficient, as well as the limiting N_{Nu}, $2f_0$, are all evaluated at T_s, while N_{Re} and m are evaluated at $T_{0.19}$. In the above, x is the value of the exponent on T, in the expression relating the kinematic viscosity and the thermal conductivity to the absolute temperature. For argon, $x = 0.8$.

3. The experimental results confirmed that the two reference temperatures defined above gave the best agreement with the numerical analysis, but that, for design and engineering purposes, the assumption of T_∞ as the reference temperature for both k and ν would be adequate.

4. In the course of the experimental work, a simple method to measure local values of the temperature of the plasma stream was developed, based on the pyrometric measurement of the local temperature of a thin tungsten wire. To account for the variable properties of the fluid surrounding the wire, an equation was derived which, for argon, works out to

$$N_{Nu0} = 0.2417\,f_0 + 0.5633\,N_{Re}^{0.455} \quad (4)$$

where the same reference temperatures as were used in connection with Equation (1) are again employed to estimate the values of the various parameters. The values of the heat transfer coefficients calculated from Equation (4) were almost identical with those experimentally obtained by Collis and Williams (1969), when modified for argon. This agreement reconfirms the concept of using a variable-property limiting Nusselt number and the reference temperature $T_{0.19}$ for evaluating the Reynolds number.

In most solids-gas plasma processes, the rate-controlling step appears to be the rate of heat transfer to the individual particles. An accurate knowledge of the heat transfer rate is, therefore, necessary for the reliable design of such devices. Practically all the experimental studies on heat transfer to spheres reported in the literature were carried out at relatively low temperatures (less than 1,000 K) where variations in the fluid properties are small and could be accounted for by choosing a reference mean film temperature. In our recent theoretical study of this situation (Sayegh and Gauvin, 1979) we show that this procedure could not be used for large temperature differences. From the numerical analysis presented in this study, a correlation was proposed, which is given by Equation (1).

A review of the literature on this subject is presented in the theoretical paper mentioned above, and it will not be repeated here. It showed that there existed virtually no experimental data on pure heat transfer against which Equation (1) could be tested. The objective our present investigation is, therefore, to provide experimental evidence in support of the theoretical predictions of this correlation.

Briefly summarized, the experimental approach consists of placing stationary spheres of polished molybdenum of various diameters in an argon plasma jet of known characteristics (velocity, temperature and pressure). The surface temperature of the sphere could be measured pyrometrically with excellent accuracy. We developed a special technique to measure the local values of the plasma temperature, based on the measurement of the temperature of a thin tungsten wire. A pitot microprobe is used to determine the local plasma velocities, in conjunction with an appropriate consideration of the special conditions of the flow. The experimental forced-convection heat transfer coefficient could then be calculated from a simple heat balance on the sphere.

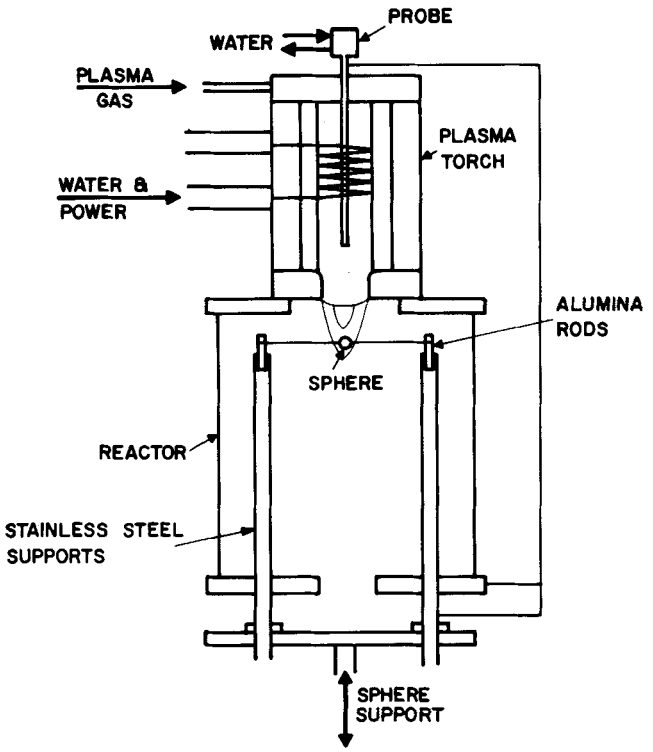

Figure 1. Schematic diagram of experimental apparatus.

APPARATUS

The apparatus in use here consists of a plasma torch, a test chamber and a sphere support assembly (Figure 1). The confinement of the plasma jet in a test chamber is necessary to avoid contamination of the plasma with entrained air from the surroundings, and to prevent rapid oxidation of the hot molybdenum spheres.

The plasma is generated in a radio-frequency induction torch operating at 4.5 MHz and 3-4 KV. Cold argon gas, fed at the top, is heated up and ionized in the coil section of the torch. The gas flows inside a quartz tube, 40 mm in diameter, which separates it from the coil. The plasma gas leaves the torch as a jet through a constricting nozzle, 25 mm in diameter. All parts of the torch are water-cooled. Power input to the high-voltage power supply is of the order of 6 KVA, of which only 30-40% was actually going to the argon plasma. The rest is carried away by the cooling water.

The test chamber consists of a pyrex glass tube, 150 mm in diameter and 250 mm long. It is equipped at both ends with brass flanges. The orifice of the inlet flange is 77 mm in diameter, and that of the outlet flange, 25 mm. The bottom of the outlet flange has two small openings, located diametrically opposite to each other and 125 mm apart, to accommodate the sphere support legs which passes through them.

The sphere assembly consists of the metal sphere, two vertical support rods and a moving platform. Three different sphere sizes are used, 2.2, 3.3 and 5.6 mm in diameter, respectively. The spheres were accurately machined from high-purity molybdenum rods. Molybdenum was selected for several reasons: (a) high melting point (2,833 K), (b) ease of machining, (c) known emissivity (as a pure metal) and most importantly (d) the high volatility of its oxide. The slight oxidation of the sphere at the end of one run and subsequent evaporation of the oxide in a following run gives the sphere a highly polished surface and frees it of any roughness or scratches caused during machining. Maintaining a very clean surface is very essential for the reproducibility of the measurements and for estimating the radiation losses from the sphere.

The spheres all supported horizontally by a thin tungsten wire passing through the axis of the sphere. The diameter of the wire is 0.25 mm for the medium and large spheres and 0.125 mm for the small sphere. Two vertical stainless steel tubes, 3 mm in diameter and over 100 mm apart holds the support wire in place. The lower ends of the rods are attached to an insulating plate supported on an adjustable jack. The sphere and support are introduced to the chamber through the bottom flange. Their level is adjusted by raising or lowering the jack. Four hair-lines, drawn 90° apart on the outside of the chamber, are used to align the sphere along the jet axis.

MEASUREMENT TECHNIQUES

The three variables for calculating the heat transfer rates to the sphere are the sphere temperature, the gas temperature and the gas velocity. Techniques of measuring these follow.

The sphere temperature is measured by means of a high-resolution pyrometer* that permitted measurements with object sizes as small as 0.1 mm. The filament of the pyrometer is focused on the equator portion of the sphere. Pyrometer ammeter readings are pre-calibrated to indicate the temperature of a black body that has the same brightness as the pyrometer filament, when a specific current is passed through the latter. Calibration is carried out at a single wave length, usually 0.65 micron. Radiation from real bodies and, consequently their brightness temperature, are both lower than those from a black body. To correct for this the following equation was used

$$1/T - 1/T_b = \lambda/C \ln \epsilon_\lambda \qquad (5)$$

The value of C is 14.38 mm·K. A knowledge of the variation of the spectral emissivity of the surface is necessary for the pyrometer correction. The spectral emissivity values for tungsten are taken from Kovalev (1970), Latyev (1969) and Sadykov (1965) and for molybdenum, Makarenko's (1970) results were used.

THE GAS TEMPERATURE

An attempt was first made to measure the gas temperature by means of thermocouples. This method had to be abandoned, however, due to arcing. Arcing took place between the plasma gas and any conducting object that was placed inside the chamber and was large enough to act as a ground. Then, we decided to discover the gas temperature by measuring the temperature of a small object suspended in the flow at the desired location. Accordingly, a thin tungsten wire, 0.25 mm in diameter, is held horizontally and perpendicular to the jet axis by the same method of support as that of the sphere. The temperature of the wire at its center (at the jet axis) is measured with the high-resolution optical pyrometer. In this situation, the temperature of the wire is always lower than the actual temperature of the gas, owing to radiation and conduction losses from the wire. To evaluate the magnitude of this difference, a heat balance is made on the wire, thus

Q(convection to wire) + Q(radiation from plasma to wire)

* Pyro Micro-Optical Pyrometer, Pyrometer Instrument Co. Inc., Northvale, N.J.

$= Q$(radiation from wire) + Q(conduction losses from wire) (6)

or:

$$(h_w)(\pi Ddl)(T_\infty - T_w) + (\epsilon_w \alpha_w \sigma)(\pi Ddl/2)(T_\infty^4 - T_w^4) = (\epsilon_w \sigma)(\pi Ddl)(T_w^4 - T^4_{\text{wall}}) - (\pi D^2/4)[k_w(dT/dl)_{l=1+dl} - k_w(dT/dl)_{l=1}] \quad (7)$$

In this equation, only the top part of the wire is assumed to be subjected to plasma radiation. Noting that the latter, as well as the conduction losses from the wire, are very small compared to the other terms, and neglecting the fourth power of the lower temperature in the radiation terms for the same reason, Equation (7) simplifies to

$$T_\infty = \epsilon_w \sigma T_w^4 / h_w + T_w \quad (8)$$

To evaluate T_∞, we must know the convective heat transfer rates to thin wires, for conditions where an appreciable temperature difference between the wire and the gas exists. An extensive literature review on this subject can be found in Sayegh's thesis (1977) and will not be repeated here. Suffice it to note that the more reliable experimental results were those reported by Collis and Williams (1959). However, their experiments were carried out on heat transfer from a hot wire to a colder gas, and the applicability of their results to the reverse situation has not been verified. On the other hand, Woo (1970) obtained numerical results for local and overall Nusselt numbers around *infinite* cylinders for constant-property fluids in the Reynolds number range of 2 to 175. His results will now be modified to include the effect of variable fluid properties. Woo's results for heat transfer to cylinders in air in the range $2 < N_{Re} < 40$ can be correlated by the following equation

$$N_{Nu} = 0.2496 + 0.5817\, N_{Re}^{0.455} \quad (9)$$

For spheres, the effects of large variations in fluid properties were accounted for by the use of Equations (1), (2) and (3). Assuming that the effects of variable properties are similar for spheres and cylinders, then Equation (9), for variable-property fluids, becomes

$$N_{Nu0} = 0.2496\, f_0 + 0.5817\, N_{Re_{0.19}}^{0.455} \quad (10)$$

The general form of heat transfer correlations for cylinders is

$$N_{Nu} = (A + BN_{Re}^n) N_{Pr}^m \quad (11)$$

and m is between 0.3 and 1/3. To convert a correlation obtained in air to one applicable for argon, the equation is multiplied by the Prandtl number ratio to the power m. For argon, Equation (11) becomes

$$N_{Nu0} = 0.2417\, f_0 + 0.5633\, N_{Re_{0.19}}^{0.455} \quad (12)$$

And, f_0 in this equation is calculated from Equation (3). The reference temperatures are the same as those used with Equation (1).

Values of the heat transfer coefficients calculated from Equation (12) are almost identical to those obtained from the Collis and Williams experimental correlation, modified for argon. This agreement reconfirms the concept of using variable-property limiting Nusselt number and the reference temperature $T_{0.19}$ for evaluating the Reynolds number.

Finally, the total hemispherical emissivity values for tungsten, ϵ_w, used in Equation (8) are those given by Logunov (1969) and Sadykov (1965). The tungsten in the wire is of ultra-high purity, and any oxide formed between the experimental runs is immediately vaporized upon exposure to the argon plasma.

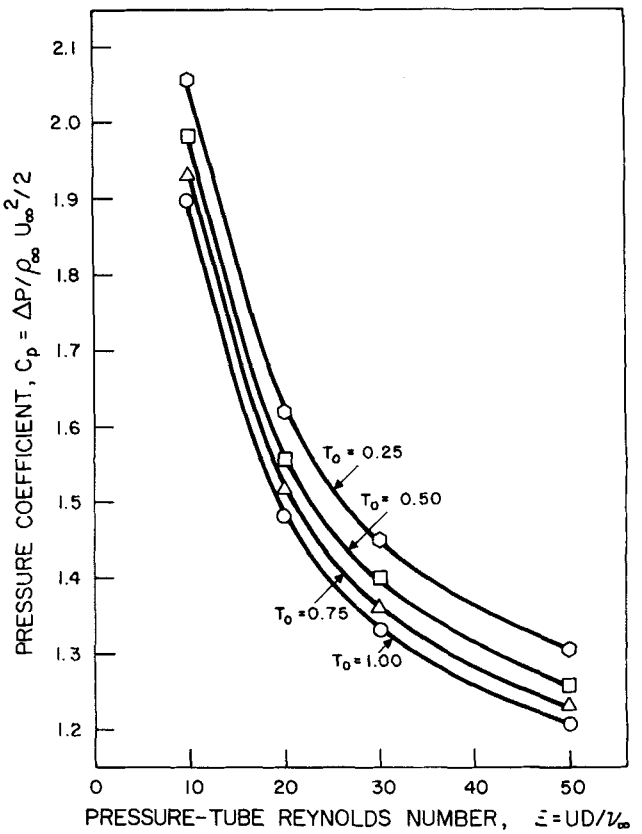

Figure 2. Effect of Reynolds number and temperature ratio on pitot-tube pressure coefficient.

THE GAS VELOCITY

The axial velocity of the plasma jet was measured by means of total pressure and static pressure microprobes. The probes were not cooled so as to keep their size (and interference with the flow) down to a minimum. The probes consist of two parts, a 65 mm long molybdenum tip and a 400 mm long stainless steel stem. The probes are round-nosed, 3.2 mm in diameter with a 1.6 mm inside bore. The taps on the static pressure probe consist of four holes, 0.5 mm in diameter, located 26 mm down from the closed nose. The temperature of the nose is measured with an optical pyrometer. Total and static pressures are measured in separate runs by means of capacitance-type differential pressure transducer. The transducer is able to indicate pressure differences as low as 10^{-5} mm Hg. One tap of the transducer is kept open to the atmosphere. The probes are introduced from the bottom of the chamber and aligned vertically, along the axis of the jet. The lower end of the probe is attached to a plexiglass platform, which is moved up and down with a manual jack.

For isothermal, high Reynolds number flows, the pitot tube equation, as derived from Bernoulli's equation, is

$$U = \sqrt{2(P_t - P_\infty)/\rho} \quad (13)$$

This equation is obtained by assuming potential flow, where the effect of viscosity is neglected. At a low Revnolds number and/or nonisothermal conditions, Equation (13) modifies to:

$$C_p = (P_t - P_\infty)/(\rho_\infty U_\infty^2/2) \quad (14)$$

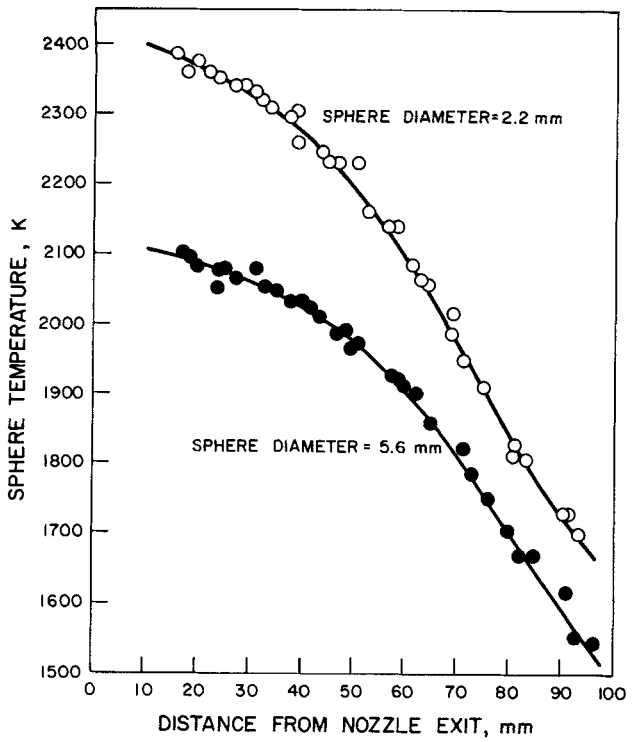

Figure 3. Variation of 2.2 mm and 5.6 mm sphere temperature with distance from nozzle exit (6 KVA, 0.72 g/s argon)

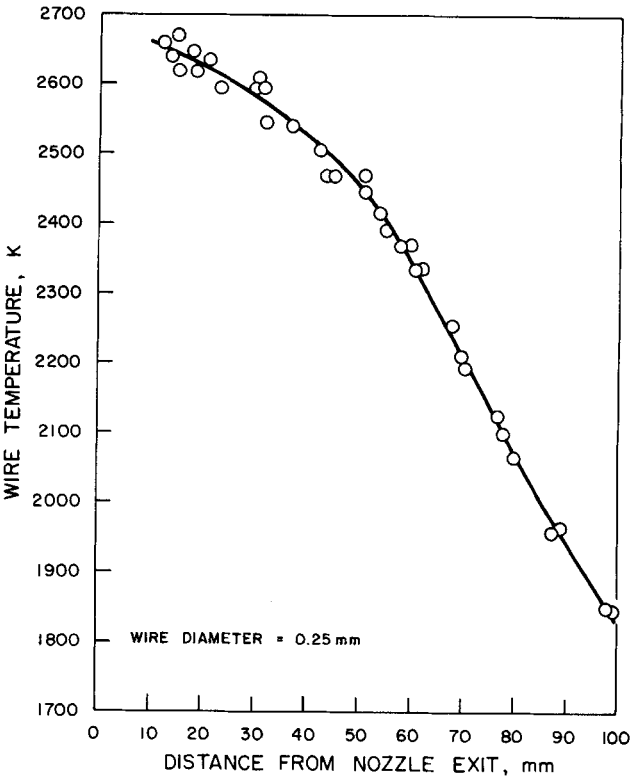

Figure 4. Variation of 0.25 mm wire temperature with distance from nozzle exit (6 KVA, 0.72 g/s argon).

The value of C_p depends on the Reynolds number of the pressure probe and on the flow and temperature conditions upstream from the probe. Chue (1975) reviewed experimental calibrations and theoretical solutions for round- and square-nosed pitot tubes at low Reynolds numbers. He concludes that for the low Reynolds range, corrections based on theoretical solutions are quite adequate for hemispherical-nose probes, irrespective of their orifice size, provided it lies in the range $0.2 < d/D < 0.74$.

We calculated the surface pressure distributions over a sphere at different Reynolds numbers and temperature conditions by solving the momentum and energy equations simultaneously. Details of these solutions are presented in the theoretical paper (Sayegh and Gauvin 1979). Comparing the pressure at the frontal stagnation point, for constant-property flow, with experimental C_p values from the literature, shows reasonable agreement. This trend is not expected to be different for nonisothermal flows since the pressure distribution over the front half of the sphere, in a variable-property flow, is very similar to that for isothermal flow—provided that the sphere temperature is not much lower than one half the value of the gas temperature. In this work, therefore, the numerical results obtained for the frontal stagnation pressure are used to evaluate C_p. Figure 2 shows the variation of C_p with the temperature ratio, at several Reynolds numbers.

EXPERIMENTAL PROCEDURE

Four different conditions of plasma power and gas flow rates are studied. The temperature range covered is $0.4 < T_s/T_\infty < 0.8$, and that of the particle Reynolds number was $10 < N_{Re_\infty} < 80$. For each of the above conditions, the total and static pressures, wire temperature and the surface temperatures of the three spheres (2.2, 3.3 and 5.6 mm in diameter, respectively) are measured at points along the axis of the plasma jet, at various distances (from 10 to 100 mm) from the nozzle exit. Each of the measurements were repeated several times to ensure reproducibility. The reproducibility of different runs, under identical conditions, is very sensitive to the metal surface conditions and, therefore, the specimens are raised to the highest position in the chamber at the beginning of each run, to ensure complete volatilization of the oxide layer.

EXPERIMENTAL DATA

The velocity of the plasma gas must be known to evaluate the heat transfer coefficient to the wire (Equation 12), and hence the temperature of the plasma jet (Equation 8). Since the velocity, in turn, requires a knowledge of the gas temperature, then these must be found simultaneously, by an iterative method. The values of the wire temperature and the stagnation pressure are taken from the smoothed curves of the experimental results, at 5 mm intervals along the axis, for the four

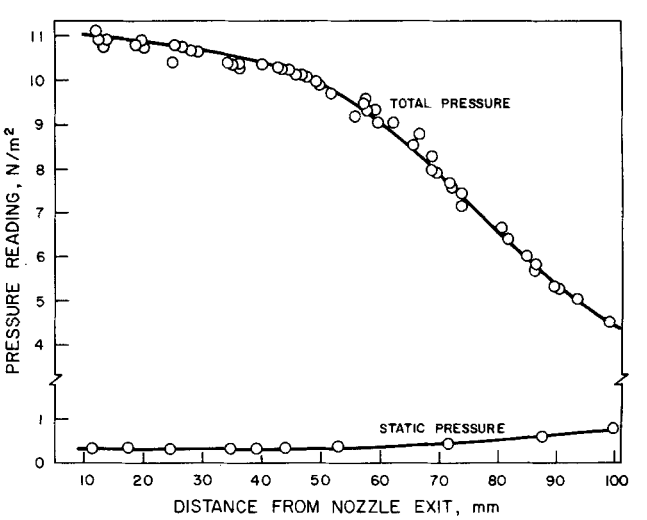

Figure 5. Variation of total and static pressures with distance from nozzle exit (6 KVA, 0.72 g/s argon).

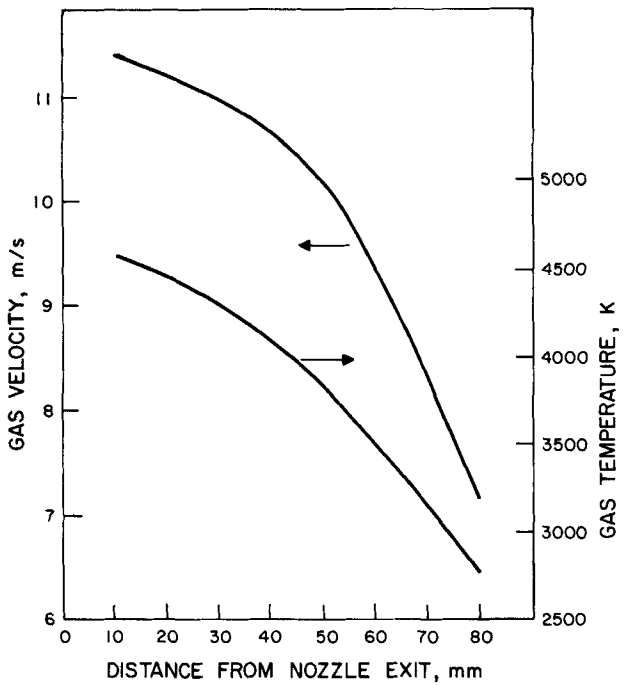

Figure 6. Gas temperature and velocity calculated from experimental data, as a function of distance from nozzle exit (6 KVA, 0.72 g/s argon).

plasma conditions. An empirical equation relating C_p to N_{Re} and T_0 is derived, based on the numerical results. Values of the velocity and temperature are assumed and then inserted in this empirical equation to give a first approximation of the gas velocity. This velocity is used in Equation (12) to find h, from which T_∞ is calculated, with the aid of Equation (8). This procedure is repeated until the difference between two consecutive values of the gas velocity and temperature are less than 0.1% of the absolute value.

The complete experimental results are available elsewhere (Sayegh 1977). Figures 3 to 6 show typical results for one power level to the plasma torch (6 kVA) and one argon flow rate (0.72 g/s argon). Figure 3 shows the variation in surface temperature of 2.2 mm and 5.6 mm spheres, with distance from the torch nozzle exit. Figure 14 shows the variations of the wire temperature, and Figure 5 those of the total and static pressures, under the same conditions. Finally, Figure 6 shows the gas temperature and the gas velocity profiles calculated from the experimental data.

CALCULATIONS OF HEAT TRANSFER TO SPHERES

A heat balance on a given sphere can now be written as follows:

$$h_s(\pi D^2)(T_\infty - T_s) + (\epsilon_s\sigma\alpha_s)(\pi D^2/2)(T_\infty^4 - T_s^4) = (\epsilon_s\sigma)(\pi D^2)(T_s^4 - T^4_{\text{wall}}) + Q_{\text{cond.}} \quad (15)$$

$Q_{\text{cond.}}$ cannot be written in an exact form since the supporting wire is in contact with the sphere at only a few discrete points. The wire temperature is always higher than that of the sphere at the points of contact. However, due to the relatively small size of the wire and the small area of contact, heat transfer by conduction from the wire to the sphere is assumed to have insignificant influence on the overall heat transfer process.

The upper half of the sphere was "seeing" a small cross-section of the plasma issuing from the torch. Based on emissivity values for argon reported by Moskvin (1968), we can show that for an average gas temperature of 6,000 K over a depth of 100 mm in the hot core, radiation from the plasma amounts to less than 0.5% of the overall heat transfer rate.

Neglecting all terms which are too small to affect the results, Equation (15) simplifies to

$$h_s = \epsilon_s\sigma T_s^4/(T_\infty - T_s) \quad (16)$$

This equation shows the direct influence of the total hemispherical emissivity on the value of the heat transfer coefficient calculated.

It is well at this point to list the assumptions which we made in the course of the experimental work, as follows:

1. The flow is uniform and unidirectional along the axis of the jet. Velocity and temperature gradients in the gas are not important.
2. Radiation from the plasma core is negligible.
3. No conduction losses through the support of the sphere.
4. No turbulence effects on the heat transfer process. The jet is assumed to be laminar.
5. Natural convection is very small compared to forced convection. It can be easily calculated that, in all experimental runs, the ratio N_{Gr}/N_{Re}^2 was $\leq 3 \times 10^{-4}$, that is, much lower than the threshold value of 0.05 found by Pei (1965). The ratio was even lower in the case of wires.

Detailed discussion of these assumptions is found in Sayegh's (1977) paper.

Equation (16) is used to calculate the forced-convection heat transfer coefficients to the three spheres. The spheres' temperatures are read from the smoothed experimental curves. Values are taken at intervals of 5 mm along the jet axis. The values of total hemispherical emissivity of molybdenum were obtained from the works of Makarenko (1970), Peletskii and Druzhinin (1969) and of Sadykov (1965).

CORRELATION AND DISCUSSION OF RESULTS

In the theoretical study (Sayegh and Gauvin 1979), the constant-property heat transfer results are correlated by the following equation, with a maximum error in the Nusselt number of less than 1% in the range $10 < Re < 100$:

$$N_{Nu} = 2 + 0.473(N_{Pr})^m(N_{Re})^{0.552} \quad (17)$$

In the case of large temperature differences between the gas and the sphere, the theoretical study proposes that the effects of the variations in physical properties could be accounted for by the following equation:

$$N_{Nu_0} = 2f_0 + 0.473(N_{Pr})^m(N_{Re})^{0.552} \quad (1)$$

where

$$m = 0.78(N_{Re})^{-0.145} \quad (2)$$

and

$$2f_0 = 2(1 - T_0^{1+x})/[(1 + x)(1 - T_0)T_0^x] \quad (3)$$

In addition to changing the value of the limiting N_{Nu} from 2 to $2f_0$, it is also necessary to use suitable reference temperatures for the thermal conductivity (in this case, the sphere temperature) and for the kinematic viscosity (in this case, $T_{0.19} = T_s + 0.19\,(T_\infty - T_s)$. In the above, x is the value of the exponent on T, in the expression relating the kinematic viscosity and the thermal conductivity to the absolute temperature.

It is important to note that the numerical analysis was carried out for the specific case of argon, where $x = 0.8$. Thus:

$$k = 1.57 \times 10^{-4}T^{0.8} \quad (\text{Jm}^{-1}\text{s}^{-1}\text{K}^{-1}) \quad (18)$$

$$\mu = 2 \times 10^{-7}T^{0.8} \quad (\text{Nsm}^{-2}) \quad (19)$$

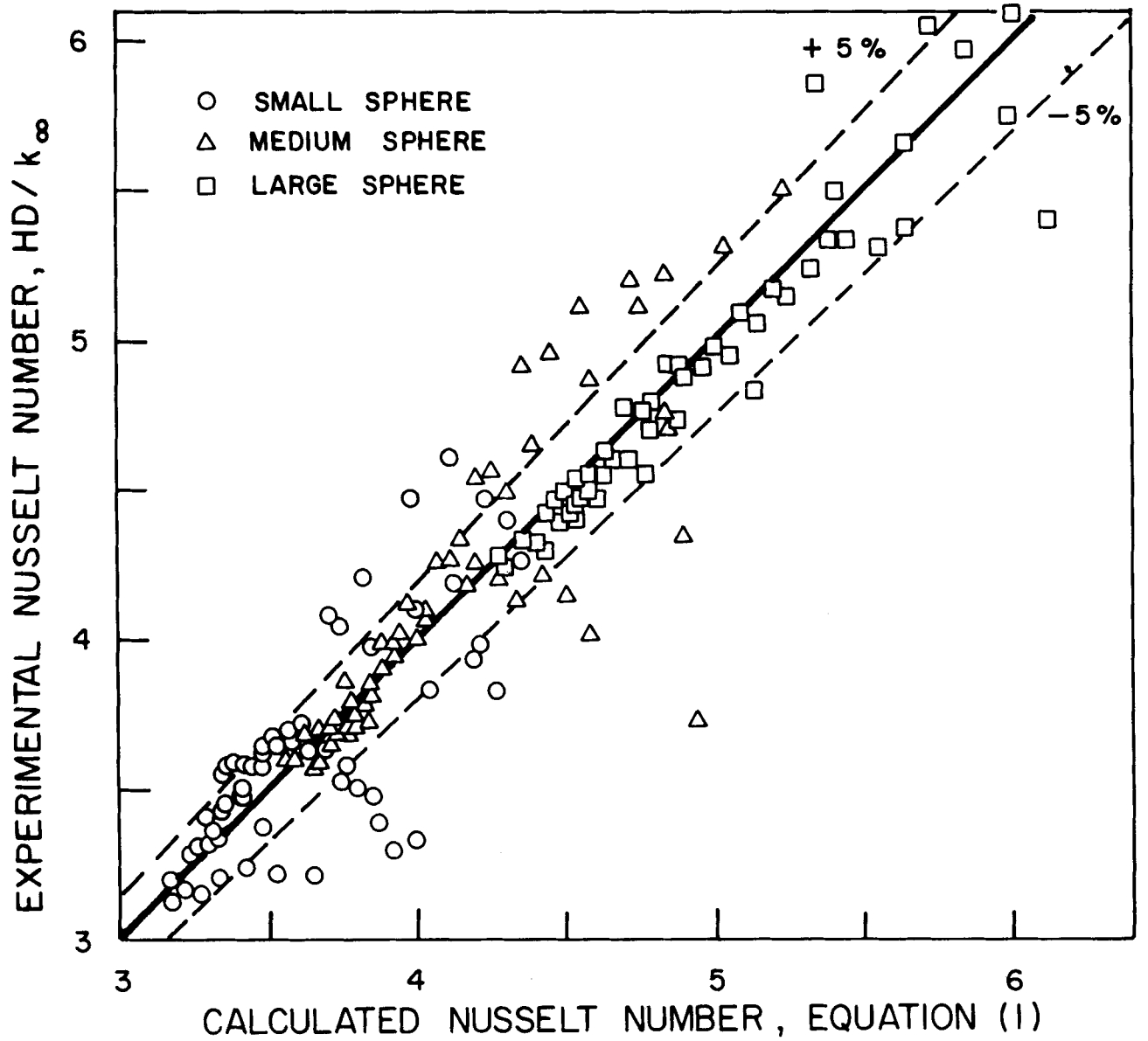

Figure 7. Comparison of experimental Nusselt number with values predicted by Equation (1).

$$\rho = 487/T \quad (\text{kg m}^{-3}) \tag{20}$$

For argon, both the specific heat and the Prandtl number (0.672) are constant with temperature (see, for example, Skrivan and von Jaskowsky 1965).

Figure 7 compares the experimental values of the Nusselt number based on the experimentally-determined values of h and the thermal conductivity evaluated at T_s, with the theoretical values based on Equation (1). Approximately 80% of the experimental points fall within ±5% of the theoretical values. The agreement is particularly good for the largest sphere (5.6 mm diameter) because of the greater accuracy of the measurements (particularly the measurement of T_s) in this case.

To further test the accuracy of Equation (1), we estimated its applicability to the experimental results, using four different reference temperatures. The standard deviation was calculated for all of the experimental points and for the individual spheres. The reference temperatures are: (a) free-stream temperature, T_∞, (b) sphere surface temperature, T_s, (c) arithmetic mean film temperature, T_m, and (d) surface temperature for evaluating the thermal conductivity and $T_{0.19}$ for the kinematic viscosity.

Table 1. Effect of Reference Temperature on the Accuracy of Heat Transfer Equation

Reference temperature	—Standard deviation (% of N_{Nu})— Overall	2.2 mm sphere	3.3 mm sphere	5.6 mm sphere
T_s	10.98	10.40	9.29	12.91
T_m	6.56	7.63	5.15	6.55
T_∞	5.06	6.70	4.36	3.48
$T_s/T_{0.19}$	4.99	6.76	4.31	3.10

The results of these tests are presented in Table 1. The reference temperatures $T_s/T_{0.19}$ gives the best results, followed by T_∞. The use of T_m gives less accurate results, while large errors are encountered when T_s is

used. The trend is particularly clear for the largest spheres, which are believed to yield the most accurate experimental results.

We regret that experimental difficulties made it impossible to investigate the behavior at T_s/T_∞ lower than 0.4 and at N_{Re} lower than 10, because it is precisely in these lower ranges that the effects of variable-property flow would be particularly felt. Examination of Equations (1) and (12), in combination with Equation (3), clearly indicates that the substitution of the constant-property limiting N_{Nu} of 2, by the variable-property $2f_0$, becomes very important at low N_{Re}. For industrial applications, where small particles (<100 μm) are generally used, low N_{Re} values in the range 1 to 10 are commonly encountered. Although it was not possible to approach these small values of N_{Re} with the stationary spheres, it is possible to do so in the case of the wires used to measure the plasma temperature. The excellent agreement between the values calculated by means of Equation (12), and the published experimental results for wires, offers additional support for the approach discussed in this paper.

Finally, for design and engineering purposes, the use of T_∞ as the reference temperature is probably adequate, at least in the range of T_s/T_∞ and N_{Re} investigated in this study.

NOTATION

A = constant
B = constant
C = constant
C_p = pitot tube pressure coefficient, dimensionless
D = diameter
dl = increment of wire length
dT/dl = temperature gradient along the wire
f_0 = effect of variable properties on limiting Nusselt number defined in Equation (3)
h = heat transfer coefficient
k = thermal conductivity
m = exponent of Prandtl number, given by Equation (2)
N_{Nu} = Nusselt number
n = exponent on Reynolds number
P_t = total pressure at stagnation point, dimensional
P_∞ = static pressure at stagnation point, dimensional
Q = heat transfer rate
R = radius
N_{Re} = Reynolds number
T = absolute temperature, dimensional
T_0 = ratio of sphere surface to free-stream temperatures (T_s/T_∞)
T_b = brightness temperature
U = free-stream velocity
x = property exponent = 0.8 for argon, Equations (18) and (19)

Greek Letters

α = absorptivity
ϵ = total hemispherical emissivity
ϵ_λ = spectral emissivity at wavelength λ (Equation 5)
λ = wave length
μ = viscosity
ν = kinematic viscosity
ρ = density
σ = Stephan-Boltzmann constant

Subscripts

m = arithmetic mean film condition
s = sphere surface condition
w = wire surface condition
∞ = free-stream condition
0.19 = reference condition at $T_{0.19} = T_s + 0.19\ (T_\infty - T_s)$

ACKNOWLEDGMENT

The authors express their appreciation for the financial support of the National Research Council of Canada and the Ministry of Education of the Province of Quebec.

LITERATURE CITED

Bhattacharyya, D. and W. H. Gauvin, "Modelling of Heterogeneous Systems in a Plasma Jet Reactor," *AIChE J.*, **21**, 879-885 (1975).

Boulos, M. I. and W. H. Gauvin, "Powder Processing in a Plasma Jet—A Proposed Model," *Can. J. Chem. Eng.*, **52**, 355-363 (1974).

Branstetter, J. R., "Some Practical Aspects of Surface Temperature Measurement by Optical Pyrometers," NASA TN-D3604 (1966).

Chue, S. H., "Pressure Probes for Fluid Measurement," *Prog. Aerospace Sci.*, **16** (2), 147 (1975).

Collis, D. C. and M. J. Williams, "Two-Dimensional Convection from Heated Wires at Low Reynolds Numbers," *J. Fluid Mech.*, **6**, 357 (1959).

Dennis, S. C. R., J. D. A. Walker and J. D. Hudson, "Heat Transfer from a Sphere at Low Reynolds Numbers," *J. Fluid Mech.*, **60** (2), 273 (1973).

Incropera, F. P. and G. Leppert, "Flow Transition Phenomena in a Subsonic Plasma Jet," *AIAA J.*, **4** (6), 1087 (1966).

International Critical Tables, Nat. Res. Council (U.S.A.), McGraw Hill (1926).

Kovalev, I. I. and G. F. Muchnik, "Normal Spectral Emissive Power of Tungsten, Niobium, Molybdenum and Tantalum . . . ," *High Temp.*, **8** (5), 922 (1970).

Latyev, L. N., V. Ya. Chekhovskoi and E. N. Shestakov, "Experimental Determination of Emissive Power of Tungsten in the Visible Region . . . ," *High Temp.*, **7** (4), 610 (1969).

Longunov, A. V. and A. I. Kavolev, "Combined Determination of Thermal Conductivity, Electrical Resistance, and Emissivity on a Single Specimen at Temperatures of More Than 1,000°C," *High Temp.*, **7** (4), 617 (1969).

Makarenko, I. N., L. N. Trukhanova and L. P. Filippov, "Thermal Properties of Molybdenum at High Temperatures," *High Temp.*, **8** (2), 416 (1970).

Moskvin, Yu. V., "Emissivity of Some Gases at High Temperatures of 6,000-(2,000)-12,000 K," *High Temp.*, **6** (1), 1 (1968).

Pei, D. C. T., "Heat Transfer from Spheres Under Combined Forced and Natural Convection," *C.E.P. Symp. Ser.*, **61** (59), 57 (1965).

Peletskii, V. E. and V. P. Druzhinin, "Experimental Determination of Integral Hemispherical Emissivity of Molybdenum at High Temperatures," *High Temp.*, **7** (1), 60 (1969).

Richardson, P. D., "Convection from Heated Wires and Moderate and Low Reynolds Numbers," *AIAA J.*, **3** (3), 537 (1965).

Sadykov, B. S., "Temperature Dependence of the Radiating Power of Metals," *High Temp.*, **3** (3), 352 (1965).

Sayegh, N. N., "Variable Property Flow and Heat Transfer to Single Spheres in High Temperature Surroundings," Ph.D. thesis, McGill University (1977).

Sayegh, N. N. and W. H. Gauvin, "Numerical Analysis of Variable-Property Heat Transfer to a Single Sphere in High-Temperature Surroundings," *AIChE J.*, **25**, 522 (1979).

Skrivan, J. F. and W. von Jaskowsky, "Heat Transfer from Plasma to Water-Cooled Tubes," *Ind. Eng. Chem. Process Des. Dev.*, **4** (4), 371-379 (1965).

Manuscript received February 23, 1979; revision received June 20, and accepted July 10, 1979.